# Hair Cycle–Dependent Basal Cell Carcinoma Tumorigenesis in Ptc1neo67/+ Mice Exposed to Radiation

Mariateresa Mancuso, Simona Leonardi, Mirella Tanori, et al.

*Cancer Res* 2006;66:6606-6614.

# Hair Cycle–Dependent Basal Cell Carcinoma Tumorigenesis in *Ptc1*$^{neo67/+}$ Mice Exposed to Radiation

Mariateresa Mancuso,[1] Simona Leonardi,[1,3] Mirella Tanori,[1] Emanuela Pasquali,[1,3] Maria Pierdomenico,[1] Simonetta Rebessi,[1] Vincenzo Di Majo,[1] Vincenzo Covelli,[2] Simonetta Pazzaglia,[1] and Anna Saran[1]

[1]Biotechnology and [2]Radiation Protection Unit, Ente per le Nuove Tecnologie, l'Energia e l'Ambiente, CR-Casaccia, Rome, Italy and [3]Department of Experimental Oncology, Istituto Nazionale Tumori, Milan, Italy

## Abstract

**We examined the effects of hair cycle phase on basal cell carcinoma (BCC) tumorigenesis induced by radiation in mice lacking one *Patched* allele (*Ptc1*$^{neo67/+}$). Our results show that *Ptc1*$^{neo67/+}$ mouse skin irradiated in early anagen is highly susceptible to tumor induction, as a 3.2-fold incidence of visible BCC-like tumors was observed in anagen-irradiated compared with telogen-irradiated mice. Microscopic nodular BCC-like tumors were also enhanced by irradiation during active hair-follicle growth phases. Interestingly, histologic examination of the tumors revealed a qualitative difference in BCC tumorigenesis depending on hair growth phase at the time of exposure. In fact, in addition to typical BCC-like tumors, we observed development of a distinct basal cell tumor subtype characterized by anti–cytokeratin 14 and anti–smooth muscle actin reactivity. These tumors showed relatively short latency and rapid growth and were strictly dependent on age at irradiation, as they occurred only in mice irradiated in early anagen phase. Examination of anatomic and immunohistochemical relationships revealed a close relation of these tumors with the follicular outer root sheath of anagen skin. In contrast, there are strong indications for the derivation of typical, smooth muscle actin–negative BCC-like tumors from cell progenitors of interfollicular epidermis. These results underscore the role of follicular bulge stem cells and their progeny with high self-renewal capacity in the formation of basal cell tumors and contribute to clarify the relationship between target cell and tumor phenotype in BCC tumorigenesis induced by radiation.** (Cancer Res 2006; 66(13): 6606-14)

## Introduction

In the Caucasian population, one of three new cancers is a skin cancer and the vast majority are basal cell carcinomas (BCC). Despite the high incidence, mortality attributed to BCC is very low. Examples of metastasizing BCC are, in fact, extraordinarily rare (1). However, they are locally aggressive and 5% to 9% may have multiple recurrences (2).

The Patched (Ptc1) protein is a Sonic Hedgehog (Shh) receptor and negative regulator of Shh signaling. Ptc1-negative regulation is relieved on Shh binding, or after Ptc1 mutational inactivation (3). In the skin, the Shh pathway regulates hair follicle morphogenesis and growth, and Shh-inappropriate activation results in formation of BCC, classically considered a hair follicle–derived tumor (4). In vertebrates, transcriptional responses to Shh and other hedgehog proteins are mediated by downstream transcription factors of the Gli family (5). Gli1 and Gli2 act as transcriptional activators whereas Gli3 acts as a repressor. Overexpression of *Gli1* or *Gli2* in skin results in BCC-like tumor development (5, 6).

Mouse models of skin cancer in many instances are good approximations of human cancer counterparts and recapitulate the tumor-stromal interactions, angiogenesis, and the multistep nature of progression of many tumors (7). In particular, mice heterozygous for mutations in the *Ptc1* gene (8, 9) represent an important model for BCC, as they exhibit an epidermal proliferative disorder, and develop BCC-like tumors following UV (9) or ionizing radiation (10). Thus, they facilitate the identification of genetic and cellular events of BCC tumorigenesis.

Mammalian skin is maintained through adult life by stem cells that have the capacity of self-renewal and also generate one or more cell lineages of the tissue (e.g., cells giving rise to the epidermis, the hair follicles, and the sebaceous glands; refs. 11–13). A specialized region of the hair follicle, known as the bulge, is a major repository of clusters of stem cells, whereas in the interfollicular epidermis, stem cells are thought to reside as single cells (13–17). Whereas the epidermis grows continuously, hair follicles are characterized by cyclic growth that alternates periods of growth (anagen), regression (catagen), and rest (telogen) throughout life (18). Although different stem cell populations have been defined in the skin, bulge stem cells are considered the primary target in cutaneous carcinogenesis (19). Because proliferating cells are more susceptible to tumor initiation (20–22), the transient activation of follicular stem cells to proliferate at the beginning of anagen suggests that the skin may be more susceptible to BCC induction by radiation during this time period.

The synchronous hair follicle cycling of the young mouse (18) provides opportunity to study how epidermal stem cell proliferation and functionality influence BCC development. Therefore, we have exposed groups of *Ptc1*$^{neo67/+}$ mice to X-rays at different ages (3, 35, or 60 days), corresponding to periods of growth or quiescence of the follicles during the first and second hair cycles. Mice in the telogen phase of hair growth (60 days old) were also exposed at day 9 after induction of anagen by depilation. We find that not only the frequency of BCC is influenced by hair cycle phase at irradiation but also that different histologic BCC subtypes occur by irradiating the skin in particular hair cycle phases. Moreover, by examining the histochemical profile of normal skin and BCC histologic variants, we provide new insights into the relationship between target cells and BCC phenotype, strongly reinforcing the concept that the diversity of epidermal tumors reflects the range of differentiated lineages of the stem cells progeny.

**Requests for reprints:** Anna Saran, Biotechnology Unit, Ente per le Nuove Tecnologie, l'Energia e l'Ambiente, CR-Casaccia, Via Anguillarese 301, 00060 Rome, Italy. Phone: 39-06-3048-4304; Fax: 39-06-3048-3644; E-mail: saran@casaccia.enea.it.



doi:10.1158/0008-5472.CAN-05-3690

## Materials and Methods

**Animals.** A colony of mice lacking one *Ptc1* allele ($Ptc1^{neo67/+}$), derived by gene targeting of 129Sv embryonic stem cells and maintained on the outbred CD1 strain background (8), was established and genotyped in the animal facility at Ente per le Nuove Tecnologie, l'Energia e l'Ambiente-Casaccia (Rome, Italy) as described (10). Animals were housed under conventional conditions with food/water available *ad libitum* and 12-hour light cycle. Experimental protocols were reviewed by the Institutional Animal Care and Use Committee.

**Irradiation.** X-ray irradiation (half-value layer, 1.6 mmCu) was done using a Gilardoni CHF 320G X-ray generator (Gilardoni S.p.A., Mandello del Lario, Lecco, Italy) operated at 250 kVp, 15 mA, with filters of 2.0 mm Al and 0.5 mm Cu. $Ptc1^{neo67/+}$ mice of both sexes were whole-body irradiated with 3 Gy of X rays at the estimated time of the second anagen [i.e., 35 days ($n$ = 60)] or of the second telogen [i.e., 60 days ($n$ = 56)]. An additional group ($n$ = 54) was irradiated at 3 days (i.e., during the first anagen); to minimize mortality for medulloblastoma, a brain tumor highly inducible by radiation in neonatal mice (23), 3-mm-thick lead shields were accurately positioned to provide protection of mouse head during irradiation. Finally, $Ptc1^{neo67/+}$ mice ($n$ = 54) were irradiated at day 9 after induction of anagen in telogen skin by depilation. Briefly, mice in the telogen phase of hair growth (60 days old) were anesthetized and depilated on dorsal skin by hot depilatory wax (18). Twenty-seven heterozygotes were left untreated as controls.

**Histologic analysis and tumor quantification.** Mice were observed daily for their whole life span; at the first signs of morbidity, they were sacrificed and complete autopsies were done. Grossly normal appearing dorsal skin (5 $cm^2$) and any skin or other tissue tumors were fixed in 4% buffered formalin, embedded in paraffin, sectioned, and stained with H&E. Tumor variables were expressed as the percentage of mice bearing one or more macroscopic or microscopic BCC-like tumors (incidence) and the mean number of macroscopic tumors per positive mouse (multiplicity). The incidence and multiplicity of microscopic BCCs were determined by analyzing dorsal skin samples from $Ptc1^{neo67/+}$ mice ($n$ = 131) autopsied in the time interval of macroscopic BCC appearance (15-87 weeks postirradiation). To shed light on hair cycle effects on nodular BCC appearance, we evaluated the same variables on the subset of mice from the three groups that were autopsied from 15 to 30 weeks postirradiation ($n$ = 61). Briefly, three skin sections per mouse were analyzed; to ensure representative sampling, sections were recovered with intervals of 100 μm. Eighteen digital images per mouse, corresponding to 40 mm of transverse skin, were collected by IAS image processing software (Delta Sistemi, Rome, Italy) with a Nikon microscope (Eclypse E800, 4× objective). The number of independent tumors in the skin analyzed was averaged for calculation of tumor multiplicity (±SE).

**Immunohistochemistry.** Immunohistochemical analysis of tumors and normal skin was done as described (10). Antibodies included rabbit polyclonal anti–cytokeratin 14 (CK14; 1:500 dilution; BabCo, Berkeley, CA), monoclonal anti-CK15 (1:100; Abcam Ltd., Cambridge, United Kingdom), and anti–α-smooth muscle actin (SMA; 1:400; Sigma Chemical Co., St. Louis, MO).

**Loss of heterozygosity at the *Ptc1* locus.** Samples from all macroscopic BCC-like tumors and noncancerous tissue were frozen at −80°C. DNA was extracted using the Wizard SV Genomic DNA Purification System (Promega Corporation, Madison, WI). Loss of heterozygosity (LOH) analysis at the *Ptc1* locus was done by amplification and sequencing of exon 23—from genomic DNA and BCC samples—of the murine *Ptc1* gene, which holds a T/C polymorphic site at position 4016 (C, CD1 derived; T, 129Sv derived). The primers used were primer pair 8F/9R (24). Sequencing reactions were done by means of dye terminator chemistry using a Big Dye Terminator Version 3.1 Sequencing Cycle kit and a 3730 DNA Analyzer (Applied Biosystems, Foster City, CA). Loss of the CD1-derived wild-type allele in neoplastic compared with nonneoplastic tissue was considered LOH.

**RNA extraction and reverse transcription-PCR.** Total RNA was isolated from macroscopic BCC-like tumors using NucleoSpin Extract (Macherey-Nagel, Duren, Germany) and stored at −80°C until further processing. Total RNA (2 μg) was reverse transcribed using RETROscript (Ambion, Inc., Austin, TX) according to the instructions of the manufacturer. The primer pairs used were sense 5′-AGACTGCCGCTGGGATGGT-3′ and anti–sense 5′-CGATGCCGCTTGGTCACG-3′ corresponding to the *Mus musculus Gli1* cDNA, yielding a 489-bp PCR product; sense 5′-CAGAACGCGGGCTTTGGTC-3′ and anti-sense 5′-GGAATTCCGGGGTGTGGTG-3′ corresponding to the *M. musculus Gli2* cDNA, yielding a 540-bp product. In the same reaction, β-actin-specific primers giving a 500-bp product were used as internal control. Scanning of the ethidium bromide gels was done with Electrophoresis Documentation and Analysis System (EDAS 290, Eastman Kodak Co., Rochester, NY); data were analyzed for mass and molecular weight using the 1D automatic lane and band finder (Image Analysis software, Eastman Kodak). For each sample, three different PCR amplifications were done and means ± SE were calculated.

**Statistics.** Analyses were done using GraphPad Prism version 4.02 for Windows (GraphPad Software, San Diego, CA). We used the Mann-Whitney test for comparison of tumor multiplicity and Fisher's exact test for analysis of tumor incidence. All $P$ values are for two-sided tests; $P < 0.05$ was considered statistically significant.

## Results

**Evaluation of hair cycle phases.** A precise time scale for mouse postnatal hair cycle was established (18). However, to make up for possible fluctuations associated with *Ptc1* heterozygosity, genetic background, and environmental/nutritional factors, dorsal skin sections from untreated $Ptc1^{neo67/+}$ mice at postnatal day 3 (P3), P35, and P60 were analyzed. Figure 1*A* shows that at P3 (A1), ~10% of neonatal hair follicles had reached their maximal length, with location of the dermal papillae close to the s.c. muscle layer, whereas the remaining follicles showed elongation of the inner root sheath halfway up through the follicle and enlarged

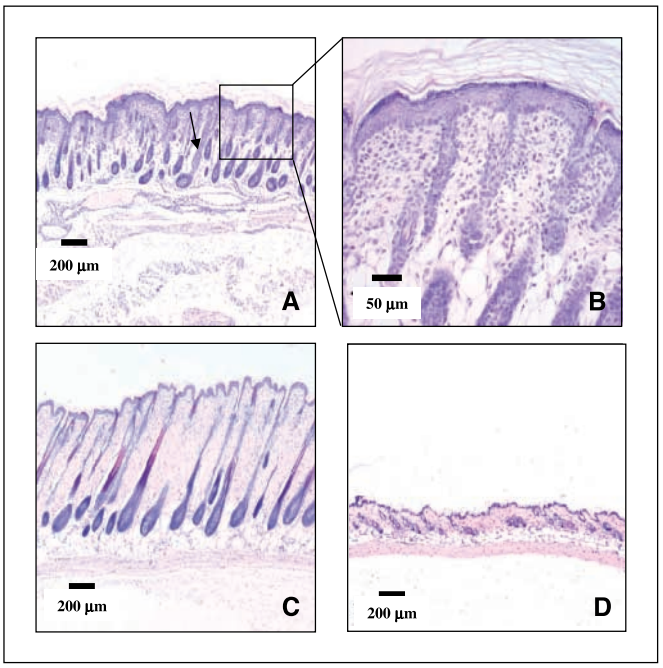


**Figure 1.** Evaluation of hair cycle in $Ptch1^{neo67/+}$ mice at different ages. *A* and *B,* histologic examination of mouse dorsal skin at P3 (A1) showed features characteristic of an early anagen phase, with few hair follicles reaching maximal length and the remaining follicles showing elongation of the inner root sheath halfway up through the follicle. *C,* at P35 (A2), the maximal extension of hair follicles and the location of the dermal papillae in the deep subcutis were indicative of a mature anagen phase. *D,* in the skin of P60 mice (T2), the follicles were fully enclosed by the dermis, indicating a quiescent phase (telogen) of the hair cycle.

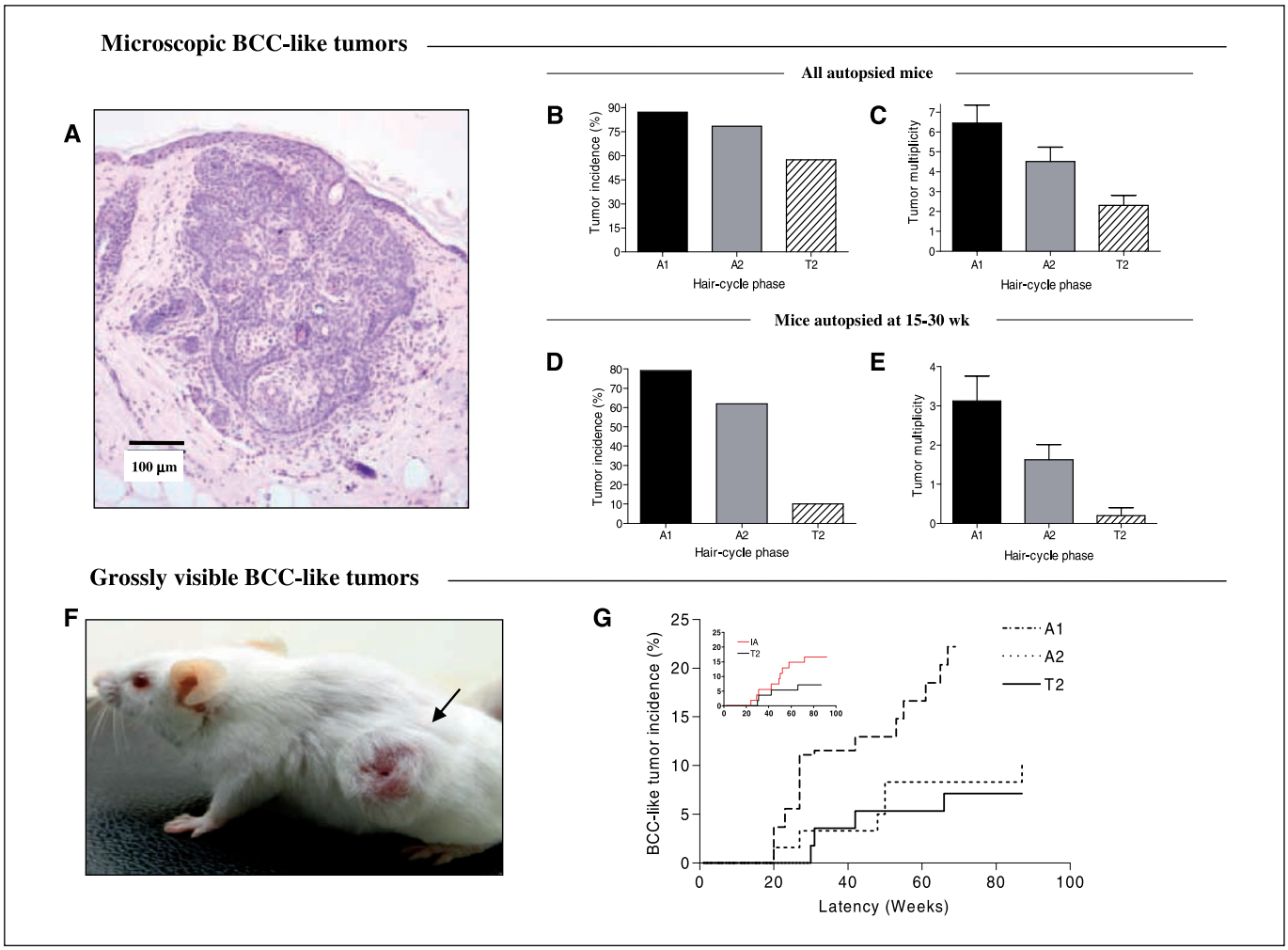


**Figure 2.** Hair cycle dependence of microscopic and grossly visible BCC-like tumors in irradiated *Ptch1*$^{neo67/+}$ mice. *A,* histology of well-circumscribed, entirely intradermic nodular BCC-like tumor, characterized by the presence of nests of basaloid cells with peripheral palisading. *B* and *C,* percent incidence and tumor multiplicity of nodular BCC evaluated in mice of the A1-irradiated, A2-irradiated, and T2-irradiated groups ($n$ = 47, 51, and 33, respectively) autopsied 15 to 87 weeks postirradiation ($n$ = 131). Differences were statistically significant between A1 and T2 and between A2 and T2 groups for both tumor incidence and multiplicity. *D* and *E,* larger differences in percent incidence and tumor multiplicity among A1-irradiated, A2-irradiated, and T2-irradiated groups ($n$ = 24, 27, and 10, respectively) were detected in mice autopsied 15 to 30 weeks postirradiation ($n$ = 61), indicating an earlier onset of nodular BCC in anagen-irradiated mice. *F,* grossly visible BCC-like tumor in irradiated *Ptch1*$^{neo67/+}$ heterozygote. *G,* incidence of macroscopic BCC-like tumors in *Ptc1*$^{neo67/+}$ mice irradiated in A1, A2, and T2 hair cycle phases. Mice irradiated in A1 showed a 3.2-fold incidence of macroscopic tumors than telogen-irradiated mice (T2) whereas a 1.4-fold incidence was observed after A2 irradiation. The difference between A1 and T2 groups was statistically significant ($P$ = 0.0313); *inset,* BCC incidence in mice irradiated at day 9 after induction of anagen in telogen skin by depilation.

bulbs (Fig. 1*B*). These features were indicative of an early anagen phase (18). At P35 (A2), the skin showed the typical architecture of a mature anagen phase, characterized by maximal extension of hair follicles, and location of the dermal papillae in the deep subcutis (Fig. 1*C*). In marked contrast, in the skin of P60 mice (T2), the follicles extended no deeper than the upper dermis and resided entirely in the dermis as small fingers of quiescent epithelial cells (Fig. 1*D*). Hair cycling resulted in remarkable changes in mouse skin thickness; in fact, A2 skin (946 μm) and A1 skin (547 μm) were 3.5-fold and 2-fold thicker than T2 skin (275 μm), respectively. Thus, the anagen skin of *Ptc1*$^{neo67/+}$ mice represents quite a different target for radiation compared with telogen skin.

**Hair cycle–dependent microscopic BCC induction.** As we previously described, irradiated *Ptc1*$^{neo67/+}$ mice develop BCC-like tumors through a multistep process that initiates with development of nodular BCCs, microscopically detectable skin tumors resembling nodular human BCC (10). Nodular BCC-like tumors were well-circumscribed, intradermic nodules of variable size and shape, characterized by the presence of nests of basaloid cells with peripheral palisading (Fig. 2*A*). We evaluated hair cycle effects on nodular-BCC induction by examining the dorsal skin of *Ptc1*$^{neo67/+}$ mice from the different irradiation groups ($n$ = 131). Nodular BCC incidence and multiplicity following irradiation in A1, A2, and T2 phases are shown in Fig. 2*B* and *C*. Both values were higher in mice irradiated in anagen phases (A1 and A2) compared with the telogen phase (T2). Tumor incidence was 87.2% in A1-irradiated, 78.4% in A2-irradiated, and 57.5% in T2-irradiated mice. These differences were statistically significant (A1 versus T2, $P$ = 0.0038; A2 versus T2, $P$ = 0.05). Tumor multiplicity was also significantly different between A1 and T2 (6.44 ± 0.9 versus 2.3 ± 0.5; $P$ = 0.0005) and between A2 and T2 groups (4.51 ± 0.72 versus 2.3 ± 0.5; $P$ = 0.0223). In addition, an earlier onset of nodular BCC in

anagen-irradiated mice was apparent by restricting this analysis to the subset of mice ($n$ = 61) autopsied early in the study (15-30 weeks postirradiation; Fig. 2*D* and *E*). In this interval, 79% of A1-irradiated and 62.9% of A2-irradiated mice developed nodular BCCs compared with 10% in mice irradiated in T2. These differences were highly statistically significant (A1 versus T2, $P$ = 0.0003; A2 versus T2, $P$ = 0.0078). Differences in tumor multiplicity between A1 and T2 (3.0 $\pm$ 0.6 versus 0.2 $\pm$ 0.2; $P$ = 0.0012) and between A2 and T2 groups (1.63 $\pm$ 0.38 versus 0.2 $\pm$ 0.2; $P$ = 0.0136) were also statistically significant. These results indicate that early BCC stages are strongly enhanced by skin irradiation during hair follicle growth.

**Hair cycle–dependent macroscopic BCC induction.** All groups of irradiated *Ptc1*$^{neo67/+}$ mice developed macroscopic BCC-like tumors. In contrast, none of the unirradiated heterozygotes developed visible BCCs during 120 weeks of observation. Tumor diameters ranged from 4 to 30 mm (Fig. 2*F*). The kinetics of tumor induction in the different groups is shown in Fig. 2*G*. A clear-cut difference between A1-irradiated and T2-irradiated mice was evident both in macroscopic BCC incidence (22.2% versus 7%;

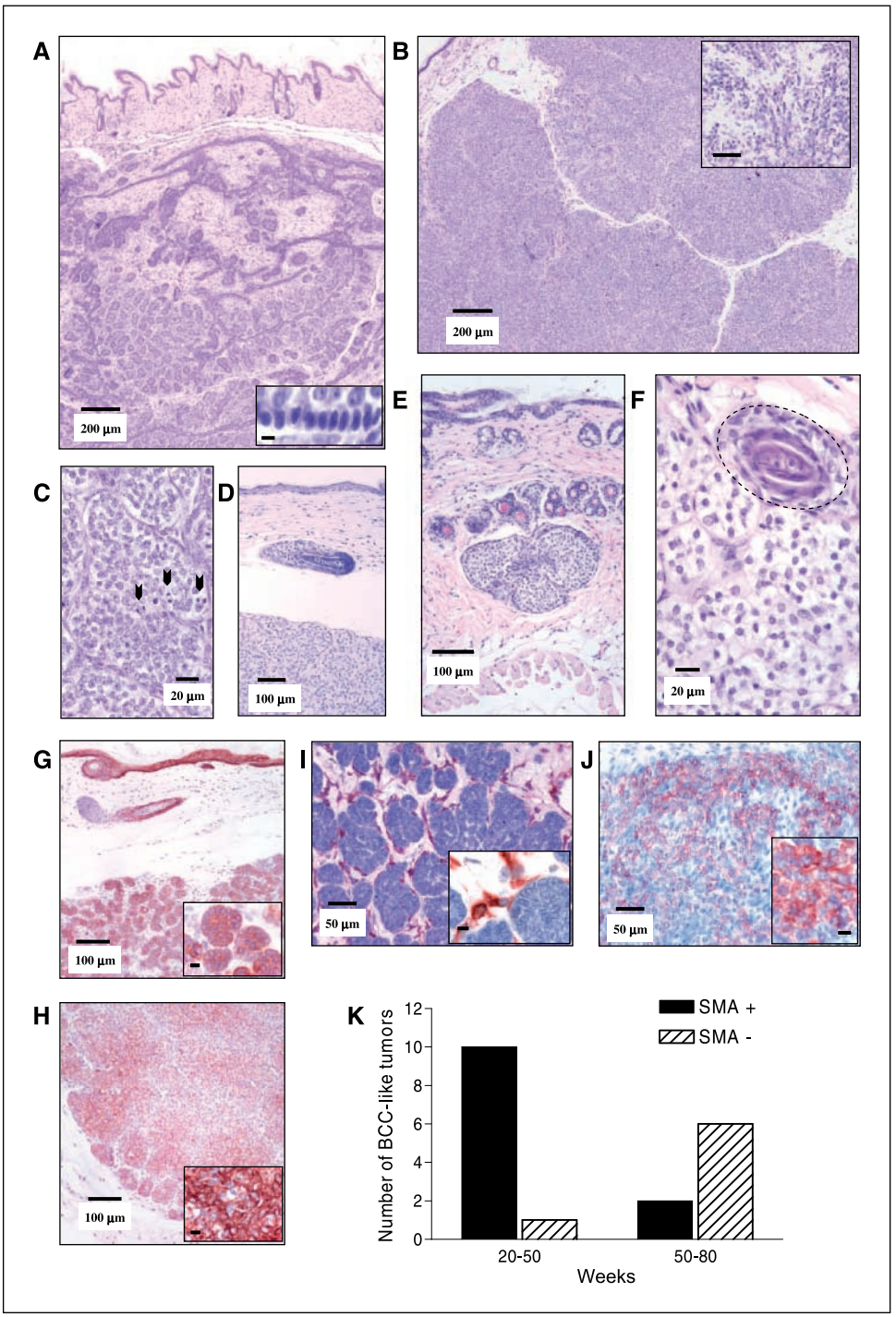


**Figure 3.** Histology, marker expression, and latency of BCC-like tumor subtypes developing in irradiated *Ptc1*$^{neo67/+}$ mice. *A,* typical BCC-like tumor characterized by the presence of irregular basaloid cell nests with typical peripheral cell palisading (*inset*) and lack of follicular differentiation, resembling human BCC. *B,* histology of BCC variant with features of myoepithelial differentiation, showing well-demarcated tumor nodules consisting of various-sized lobular nests of epithelial cells. *Inset,* areas composed of elongated or spindle-shaped cells (*bar,* 100 μm). These tumors showed basophilic nuclei, mild nuclear pleomorphism, and presence of numerous mitotic figures (*C*). *D,* striking similarity of cellular morphology in follicular outer root sheath and in BCCs with myoepithelial features, and initial phase of this histologic subtype arising in irradiated skin in the approximate location of outer root sheath development (*E*). *F,* direct connection with a developing follicle. *G* and *H,* CK14 immunoreactivity in a typical BCC-like tumor (*G*) and in BCC with myoepithelial differentiation (*H*); *insets,* bar, 8 μm. *I* and *J,* analysis of SMA expression in BCC-like tumor subtypes. *I,* note the absence of SMA immunoreactivity in typical BCC-like tumor nests and SMA presence only in the stroma surrounding the tumor nests; *inset,* bar, 8 μm. *J,* widespread positivity for SMA was detected in tumors with myoepithelial features; *inset,* bar, 8 μm. *K,* SMA-expressing basal tumors represented the vast majority (10 of 12) of the total tumors observed up to 50 weeks postirradiation. Conventional BCC-like tumors represented the prevalent subtype (6 of 7) beginning from 50 weeks postirradiation.

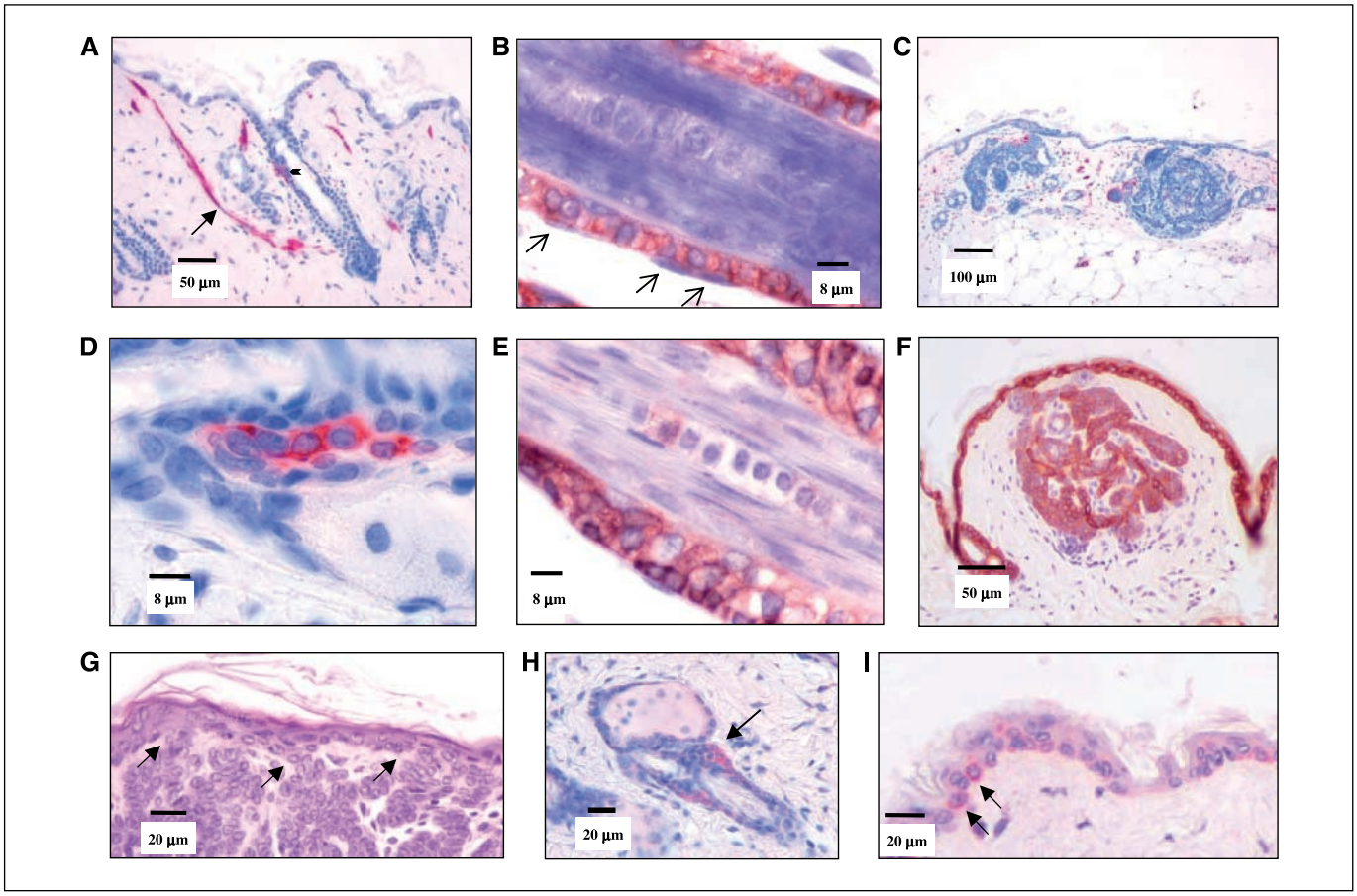


**Figure 4.** Cell lineage selection in different BCC subtypes. *A* to *D,* SMA immunoreactivity in normally appearing skin of *Ptc1*$^{neo67/+}$ mice. SMA expression was detected in the arrector pili muscles (*A, arrow*), in the bulge region (*A, arrowhead*; *D*, higher magnification), and in outer root sheath keratinocytes (*B*); SMA expression was lacking in normal keratinocytes of the basal layer (*A*), in the fibroblasts of the dermal sheath surrounding the outer root sheath (*B, arrows*), and in nodular BCCs (*C*). *E* and *F,* CK14 immunoreactivity in normally appearing skin of *Ptc1*$^{neo67/+}$. Strong CK14 reactivity was detected in outer root sheath keratinocytes (*E*) and in nodular BCCs (*F*). *G,* early-stage nodular BCCs show an intimate connection with the interfollicular epidermis. *H* and *I,* CK15 immunoreactivity in normally appearing skin of *Ptc1*$^{neo67/+}$. Strong CK15 expression was observed in the hair follicle bulge (*H*) as well as in scattered epidermal keratinocytes of the basal layer (*I*).

$P = 0.0313$) and in tumor latency (20 versus 30 weeks). Furthermore, only the mice exposed in A1 developed multiple macroscopic BCCs (tumor multiplicity = $1.6 \pm 0.51$). Similar to A1-irradiated mice, mice exposed in A2 had a short tumor latency (20 weeks) but BCC incidence in this group was only 1.4-fold compared with the T2 group (10% versus 7%). This smaller BCC enhancement is consistent with the more progressed stage of hair follicle maturation in A2 compared with A1 skin (Fig. 1*A* and *C*). Overall, the trend observed in our tumor data is supported by the fact that mice irradiated at P3 (A1) and P35 (A2) survived significantly less (median survival time: P3, 27 weeks; P35, 32 weeks) than mice irradiated at P60 (T2; 47 weeks), thus having lower chance to develop BCCs ($P < 0.0001$, P3 versus P60; $P = 0.0008$, P35 versus P60). To confirm that hair follicle cycling, rather than mere age effect, was responsible for different tumor responses, anagen was artificially induced in 60-day-old (telogen) *Ptc1*$^{neo67/+}$ mice before X-ray exposure. Histologic examination of the skin at day 9 after depilation confirmed the induction of anagen (data not shown). The results of this experimental group show a 2.4-fold increase in tumor incidence (16.7%) relative to telogen-exposed mice (Fig. 2*G, inset*), confirming a causative role of hair follicle growth in BCC tumorigenesis. Thus, ionizing radiation synergizes with *Ptc1* deficiency to produce early and advanced BCC stages in a hair cycle–dependent manner.

**Two different BCC subtypes in irradiated Ptc1**$^{neo67/+}$ **mice.** All grossly visible BCC-like tumors were macroscopically similar, appearing as well-circumscribed superficial dermal nodules (Fig. 2*F*). Histopathologically, some of the tumors were characterized by the presence of irregular basaloid cell nests with typical peripheral cell palisading and lack of characteristics of the hair follicle lineage, resembling human BCC (Fig. 3*A*; ref. 10). Interestingly, in numerous other cases, tumors had different histopathologic features, being composed by well-demarcated tumor nodules consisting of various-sized lobular nests of epithelial cells with abundant homogeneous or ground-glass pale cytoplasm, embedded in relatively scarce tumor stroma (Fig. 3*B*). Areas composed of elongated or spindle-shaped cells were present in some of the tumors (Fig. 3*B, inset*). Nuclei were basophilic and nuclear pleomorphism was mild, but mitotic figures were numerous (Fig. 3*C*). Prominent cleaving between tumor stroma and surrounding connective tissue was often observed (Fig. 3*B* and *D*); similar retraction spaces are frequently observed in human BCC nodules (5). In contrast with the typical BCC-like tumors, peripheral palisading of the cells was lacking in the tumor nests and blood vessels were scarce in the stroma surrounding the lobules (Fig. 3*B*). The peculiar morphologic characteristics of this previously undetected BCC variant were suggestive of

myoepithelial differentiation, a feature also observed in human BCC (25, 26). The cellular morphology in this murine basal tumor was strikingly similar to that in the outer root sheath, the outermost compartment of the anagen hair follicle (Fig. 3*D*). Interestingly, we occasionally observed rare initial phases of this histologic type arising in irradiated skin of *Ptc1*$^{neo67/+}$ mice in the approximate location where outer root sheath development occurs (Fig. 3*E*) and, in some cases, a direct connection with a developing follicle could be detected (Fig. 3*F*).

Immunohistochemically, typical BCC-like tumors and the new BCC variants showed strong positivity for CK14, a basal differentiation marker (Fig. 3*G* and *H*). Strong CK14 expression was also detected in epidermis and follicular outer root sheath (Fig. 3*G*). Because SMA, the major component of microfilaments controlling cell morphology and motility, is a marker of myoepithelial differentiation (27), we did immunohistochemical analysis to look for evidence of SMA expression in the tumors. Typical BCC-like tumors were uniformly negative for SMA and only the stroma surrounding the tumor nests stained positively (Fig. 3*I*). In contrast, widespread positivity for SMA was detected in tumors with myoepithelial features (Fig. 3*J*) and the spindled-cell component often showed stronger staining (not shown).

The two histologic subtypes seemed to have a nonrandom distribution in the groups. In particular, most of the tumors (12 of 19) from A1-irradiated mice were of the newly detected SMA-expressing subtype. All other tumors from this and other groups lacked SMA expression and were classified as typical BCC-like tumors based on their strong resemblance to infiltrative human BCC and on SMA-negativity (10). In addition, SMA-expressing basal tumors appeared as an earlier wave compared with typical BCC-like tumors. They had a mean latency of 26 weeks, thus representing the vast majority (10 of 12) of the total tumors observed up to 50 weeks postirradiation (Fig. 3*K*). Conventional BCC-like tumors had a later onset, with a mean latency of 51 weeks, and represented the prevalent subtype (6 of 7) beginning from 50 weeks postirradiation (Fig. 3*K*). Collectively, the results of morphologic and histochemical analysis and the different tumor behavior support classification in two distinct BCC subtypes.

**Cell lineage selection in different BCC subtypes.** Immunohistochemical profiles of the two BCC subtypes and of normal-appearing skin of *Ptc1*$^{neo67/+}$ mice help to elucidate cell lineage relationships. Consistent with the fact that actin is only sparsely found in normal epithelial cells (27), analysis of anti-SMA reactivity in normal skin showed lack of SMA expression in normal keratinocytes of the basal layer whereas SMA was detected in the arrector pili muscles and pericytes around blood vessels (Fig. 4*A*). Surprisingly, both the outer root sheath of anagen hair follicles (Fig. 4*B*) and the follicular bulge region (Fig. 4*A* and *D*) also consistently showed strong SMA expression, suggesting a relation between SMA-expressing tumors and cells of the outer root sheath and/or the bulge. SMA expression pattern in outer root sheath cells was comparable with that of CK14 (Fig. 4*B* and *E*), and SMA intracytoplasmic reactivity was clearly in association with outer root sheath keratinocytes specifically and not, as previously suggested (28), with the fibroblasts of the dermal sheath surrounding the outer root sheath, which were uniformly SMA negative (Fig. 4*B*). SMA expression in the outer root sheath and bulge was not in correlation with the *Ptc1* genotype, as similar SMA-positive staining of these regions was observed in wild-type CD1 mice (not shown).

To assess whether there was a similar correlation between early BCC stages and outer root sheath/bulge cells, as well as SMA-expressing tumors, we examined anti-SMA and anti-CK14 reactivity in nodular BCCs. These microscopic lesions uniformly showed

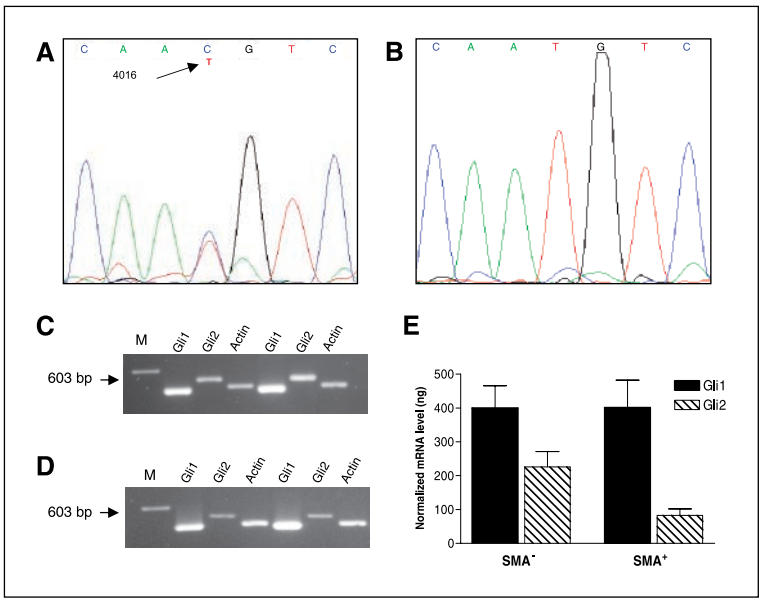


**Figure 5.** LOH analysis at the *Ptc1* locus and expression of *Gli1* and *Gli2* in BCC subtypes. *A* to *C,* representative set of electropherograms showing the results of sequencing in normal tissue (*A*) and in the two BCC subtypes (*B*). Retention of both CD1-derived and 129Sv-derived polymorphisms was observed in normal control tissue, showing retention of both *Ptc1* alleles (*A*). Loss of the CD1-derived allele and retention of the 129Sv-derived allele in typical BCC-like tumors and in the SMA-expressing variant (*B*). *C* and *D,* representative gels showing cDNAs obtained from typical BCC-like tumors (*C*) and SMA-expressing variants (*D*) amplified using *Gli1*, *Gli2*, and β-actin primers. *M,* marker [ΦX174 DNA/*Bsu*RI (*Hae*III) Marker, 9, Fermentas International, Inc., Burlington, Ontario, Canada]. *E,* normalized expression levels of *Gli1* and *Gli2* in typical BCC-like tumors (*SMA*$^-$) and SMA-expressing variants (*SMA*$^+$). Three independent PCR runs were carried out for each tumor and β-actin was used as a reference standard for all analyses to control for the amount of sample material. Data represent the ratios of final averages for BCC-like tumors of each subtype ($n$ = 5). *Bars,* SD.

intracytoplasmic reactivity for CK14 with strong staining intensity (Fig. 4*F*). Instead, similar to typical BCC-like tumors, they lacked SMA expression (Fig. 4*C*). In addition, early-stage nodular BCCs were always connected to epidermis rather than hair follicles (Fig. 4*F* and *G*). Because data from our laboratory have shown that BCC development in *Ptc1*$^{neo67/+}$ mice is a process occurring through the accumulation of genetic alterations reminiscent of that seen in colorectal cancer (10), and because only the long-term residents of the epidermis (i.e., the stem cells) have the ability to accumulate the number of genetic lesions required for tumor formation, we analyzed expression of CK15, a biochemical marker that has been shown to correlate with a less differentiated keratinocyte phenotype and is preferentially expressed in adult mouse bulge cells. We report here that the normal skin of adult *Ptc1*$^{neo67/+}$ mice shows strong CK15 expression in the hair follicle bulge, as well as in scattered epidermal keratinocytes of the basal layer (Fig. 4*H* and *I*). A similar CK15 expression pattern was observed in wild-type mice (not shown).

**Allelic imbalance analysis at the *Ptc1* locus in basal tumors.** Loss of the wild-type *Ptc1* allele was examined in both BCC histologic variants. Sequence analysis of tumor DNA to screen a T/C polymorphism in position 4016 of the *Ptc1* gene was carried out to assess the presence of the nucleotide sequence of the targeted *Ptc1* allele, derived from 129Sv embryonic stem cells, and of the wild-type allele derived from CD1 mice. We consistently detected loss of wild-type *Ptc1* and retention of the mutant allele in typical BCC-like tumors (3 of 3 from different groups) and in SMA-expressing BCCs (5 of 5 from A1-irradiated mice) but not in normal control tissue (Fig. 5*A* and *B*).

**Expression of *Gli 1* and *Gli 2* in tumor cells.** Expression of *Gli* transcriptional targets of Shh signaling is often up-regulated in BCCs, and overexpression of *Gli1* and *Gli2* in mouse epidermis induces BCC-like tumors (5, 6). In addition, the levels of hedgehog pathway activation are major determinants of tumor phenotype (29). Therefore, we next quantified by reverse transcription-PCR *Gli1* and *Gli2* mRNA levels in typical BCC-like tumors ($n$ = 5) and in SMA-expressing BCC variants ($n$ = 5; Fig. 5*C* and *D*). Whereas *Gli1* was expressed to the same extent in the two subtypes, typical BCC-like tumors showed a 2.7-fold increase in *Gli2* mRNA expression (Fig. 5*E*), suggesting that increased and sustained *Gli2* expression is a stronger requirement for growth of typical BCC-like tumors compared with SMA-expressing BCCs.

## Discussion

**Hair cycle dependence of radiation-induced BCC tumorigenesis.** Ionizing radiation is a well-known cytotoxic/genotoxic agent that increases cancer risk both in humans and in mice and has long been known to cause skin cancer, especially BCC (30, 31). In this study, using a recently established mouse model of radiation-induced BCC tumorigenesis, we have shown that the yield of basaloid tumors after irradiation of *Ptc1*$^{neo67/+}$ mice can be significantly affected by the growth or quiescence of the follicles during exposure. Anagen skin, in fact, developed significantly more early and advanced BCC-like tumors than telogen skin after irradiation. The shortened latency for macroscopic and microscopic BCC-like tumors in anagen-irradiated groups and the occurrence of multiple macroscopic tumors only in mice irradiated in early anagen (A1) further support hair cycle–related susceptibility. These results are strengthened by the fact that mice irradiated in neonatal (P3) or young age (P35) survived less than mice irradiated as adults (P60), and thus had lower chance to develop microscopic or visible BCC-like tumors. Finally, induction of anagen in telogen skin considerably increased radiation susceptibility and induced excess BCCs in *Ptc1*$^{neo67/+}$ mice, confirming that BCC tumorigenesis and its age effect are dependent on the developmental changes in proliferation/differentiation status of the skin and its highly sensitive hair follicles.

Because cellular radiosensitivity is increased in proliferating cells (20, 22), we suggest that such higher BCC susceptibility is due to the transient proliferation of follicular stem cells during anagen and to the drastic increase in number of rapidly cycling committed progenitors, or transit-amplifying cells, in individual hair follicles at this stage (32). This hypothesis is consistent with our finding that in A2-irradiated mice, the macroscopic tumor yield was only modestly increased over the T2 group, and enhancement of microscopic tumors, although significant, was less pronounced than in the A1 group. In fact, in A1 skin, only a minority of neonatal hair follicles has reached maximal length, compared with A2 skin characterized by maximal extension of hair follicles and postmitotic outer root sheath (Fig. 1*C*). Although hair cycle–dependent susceptibility to squamous cell papillomas developing after one-stage or two-stage chemical carcinogenesis has been reported (33), our findings show for the first time that X-ray irradiation enhances BCC development in a hair cycle–dependent manner and underscore the role of bulge stem cells in formation of basal tumors.

**Development of different BCC subtypes in irradiated *Ptc1*$^{neo67/+}$ mice.** An unexpected and interesting outcome of our experiments was the qualitative difference in tumorigenicity depending on hair cycle phase at irradiation. In fact, we observed development of two different histologic BCC subtypes, both closely mimicking human tumor counterparts as regards morphologic and histochemical features, local invasiveness, and lack of metastatic spreading. BCC-like tumors resembling human BCC, previously induced in this mouse model after exposure to UV or ionizing radiation (9, 10), showed delayed onset, slow growth rate, and development through a multistep process in which nodular and infiltrative BCC-like tumors represent different stages of tumor progression. In addition, they were uniformly CK14 positive and SMA negative.

Here, for the first time, we show a high incidence of BCC-like tumors showing histologic features reminiscent of myoepithelial differentiation, occasionally described in sporadic human BCC, and SMA immunoreactivity. Interestingly, SMA-expressing BCC-like tumors had a peculiar biological behavior, characterized by fast growth rate and lack of identifiable precursor lesions, as shown by the virtually complete absence of early SMA-expressing lesions in routine microscopic observation of irradiated skin. They were also strictly hair cycle dependent, occurring only in mice irradiated in early anagen (A1), and had a mean latency considerably shorter compared with the conventional BCC subtype (26 versus 51 weeks).

**Origin of BCC subtypes.** An important issue is the differentiation of the starting point of tumorigenesis. To this end, morphologic and immunohistochemical analysis of tumors and of normal skin from experimental mice has provided several important cues about the nature of cellular targets for the different tumors arising in irradiated *Ptc1*$^{neo67/+}$ mice.

Our data suggest a critical role for the interfollicular epidermis in formation of conventional BCC-like tumors. The close anatomic connection of interfollicular epidermis with nodular BCCs—precursors of conventional BCC-like tumors—suggests that these

tumors derive from interfollicular epidermis as epidermal downgrowths into the underlying dermis (Fig. 4*H*). Similarly, previous studies have shown that the epithelium of follicular hamartomas, also arising in association with deregulated Shh signaling, is connected to epidermis rather than hair follicles both in humans and in mice (29).

We show here that CK15-expressing epidermal cells are present in adult epidermis of *Ptc1*$^{neo67/+}$ mice, consistent with recent results showing that label-retaining cells are found within the basal layer of the epidermis in addition to the hair follicle bulge (34). Because CK15 is considered a biochemical marker of epidermal stem cells (15), interfollicular CK15-expressing cells may represent the target for nodular BCC and its progressed stage, the macroscopic typical BCC. Although CK15 is reported as a good intracellular marker for both the stem and transit-amplifying population in human skin (35), it cannot distinguish between keratinocyte stem cells and the transit-amplifying progeny of bulge cells in CK15-positive epidermal cells. Because epidermis growth is continuous rather than cyclical, the strong hair cycle–dependent enhancement of nodular BCC—the early-stage lesion for the macroscopic typical BCC-like tumor—suggests a contribution of follicular bulge stem cells to this tumor subtype. This is consistent with earlier results showing that bulge epidermal stem cells are not only responsible for forming the lower hair follicle but may be also a major source of progenitor cells that give rise to the interfollicular, cornified epithelium (11).

A distinct cell-target population can be postulated for SMA-expressing, nonconventional BCC-like tumors, which could explain their distinctive biological features. Based on morphologic and immunohistochemical evidence, we propose that this population is represented by the outer root sheath progenitors, which undergo maximal transient proliferation during anagen to generate a critical part of the new hair follicle structure, and have been shown to express potential markers of hair follicle stem cells (36).

Thus, our findings are suggestive of a different cellular origin of the two BCC subtypes. However, at this stage, we cannot exclude that both types of BCCs arise from the same lineage (i.e., from bulge stem cell progeny) and what distinguishes them is that they arise from cells in different states of differentiation.

The biological significance of the presence of SMA in outer root sheath cells remains unknown. Because actin is the predominant component in contractile microfilaments, which are responsible for cell motility and transport, SMA may play a role in cell migration and/or morphologic changes in the lower portion of the follicle during hair cycle (28). On the other hand, because the follicular bulge region also showed SMA immunoreactivity (Fig. 4*A*), it is possible that SMA-expressing cells in the outer root sheath (and possibly in outer root sheath-related tumors) derive from SMA-expressing putative stem cells of the bulge area. As SMA expression was reported in smooth muscle progenitor cells (37), SMA expression in the bulge might be analogous to the reported expression of nestin, the neural stem cell marker, in bulge stem cells (36). Indeed, nestin-expressing cells isolated from the mouse hair-follicle bulge area were shown to be able to differentiate *in vitro* into many cell lineages, including smooth muscle cells (38). Our finding that cells of the bulge area express SMA *in vivo* strongly supports the *in vivo* multipotency of hair follicle stem cells.

**Analysis of *Ptc1* allelic status.** Analogously to human BCCs, LOH at the *Ptc1* locus is implicated in BCC tumorigenesis in *Ptc1*$^{neo67/+}$ mice and has been reported in previous experiments with UV (9) or ionizing radiation (10, 39). To determine whether the different histologic features of BCC subtypes were associated with altered allelic patterns at the *Ptc1* locus, we examined *Ptc1* allelic imbalance in DNAs from both BCC variants. We show that all tumors analyzed are characterized by loss of the remaining normal *Ptc1* allele, confirming that complete loss of *Ptc1* function is a key event in BCC tumorigenesis regardless of the differentiation route or cellular target involved in tumor formation.

**Expression of *Gli1* and *Gli2* in BCC subtypes.** Several mouse models support the concept that aberrant Shh pathway activation is sufficient to drive development of BCC-like tumors (5, 6, 9, 40, 41), and recent results indicate that different levels of Shh signaling activity results in formation of different tumor types in skin (29). Uncontrolled Shh signaling associated with BCC development is mediated primarily through the Gli family of transcription factors and BCC-like tumors are induced by overexpression of *Gli1* and *Gli2* in mouse epidermis (5, 6). Particularly, *Gli1* overexpression results in development of multiple types of skin tumors of basal cell origin, only a minority of which are BCCs (5). In contrast, overexpression of *Gli2* causes spontaneous development of multiple BCCs (6, 41). This is interesting in light of our results of expression of *Gli1* and *Gli2* in radiation-induced typical BCC-like tumors and SMA-expressing variants. Whereas *Gli1* was similarly expressed in both tumor subtypes, *Gli2* mRNA expression was significantly higher in typical BCC-like tumors. Whether this reflects a different expression level of the two Shh-signaling mediators in the target cell populations involved in tumor formation or, rather, a dependence of tumor phenotype on the level of Shh activity regardless of the tumor progenitor cells remains to be established. However, based on our results and on recent findings showing that *Gli2*, but not *Gli1* mRNA, is expressed in normal interfollicular epidermis (42), we favor the hypothesis that differential *Gli2* expression in BCC subtypes developing in irradiated *Ptc1*$^{neo67/+}$ mice reflects the expansion of different cellular targets and/or progenitor cells at different stages of hair follicle maturation.

**Conclusions.** The studies outlined here support the concept that BCC tumorigenesis can be strongly affected by the hair growth cycle and that the tumor yield, histologic type, and tumor behavior are dependent on the follicular phase during which tumor initiation by radiation occurs. By showing that the time periods of susceptibility to different BCC subtypes coincide with the transient proliferation of stem cells/committed progenitors, and by defining histochemical relationships between putative target cells and BCC variants, our results contribute to clarify the lineage selection observed in tumors. Finally, by delineating a new smooth muscle–related histochemical profile for bulge and outer root sheath cells, we extend previous findings of neural stem cell marker expression in bulge/outer root sheath progenitors (36) and strengthen the hypothesis that these cells represent a multipotent adult stem-cell compartment that can easily generate cells of more than one embryonic lineage.

## Acknowledgments

Received 10/12/2005; revised 3/31/2006; accepted 4/26/2006.

**Grant support:** Commission of the European Communities, Association Contract FI6R-CT-2003-508842 RISC-RAD.

The costs of publication of this article were defrayed in part by the payment of page charges. This article must therefore be hereby marked *advertisement* in accordance with 18 U.S.C. Section 1734 solely to indicate this fact.

We thank Orsio Allegrucci for assistance in handling and treating the mice.

## References


1. Tavin E, Persky MS, Jacobs J. Metastatic basal cell carcinoma of the head and neck. Laryngoscope 1995; 105:814–7.
2. Miller SJ. Biology of basal cell carcinoma (part I). J Am Acad Dermatol 1991;24:1–18.
3. Ruiz i Altaba A, Sanchez P, Dahmane N. Gli and hedgehog in cancer: tumours, embryos and stem cells. Nat Rev Cancer 2002;2:361–72.
4. Callahan CA, Oro AE. Monstrous attempts at adnexogenesis: regulating hair follicle progenitors through Sonic hedgehog signaling. Curr Opin Genet Dev 2001; 11:541–6.
5. Nilsson M, Unden AB, Krause D, et al. Induction of basal cell carcinomas and trichoepitheliomas in mice overexpressing GLI-1. Proc Natl Acad Sci U S A 2000;97: 3438–43.
6. Grachtchouk M, Mo R, Yu S, et al. Basal cell carcinomas in mice overexpressing Gli2 in skin. Nat Genet 2000;24:216–7.
7. Van Dyke T, Jacks T. Cancer modeling in the modern era: progress and challanges. Cell 2002;108:135–44.
8. Hahn H, Wojnowski L, Zimmer AM, Hall J, Miller G, Zimmer A. Rhabdomyosarcomas and radiation hypersensitivity in a mouse model of Gorlin syndrome. Nat Med 1998;4:619–22.
9. Aszterbaum M, Epstein J, Oro A, et al. Ultraviolet and ionizing radiation enhance the growth of BCCs and trichoblastomas in patched heterozygous knockout mice. Nat Med 1999;5:1285–91.
10. Mancuso M, Pazzaglia S, Tanori M, et al. Basal cell carcinoma and its development: insights from radiation induced tumors in Ptch1 deficient mice. Cancer Res 2004;64:934–41.
11. Taylor G, Lehrer MS, Jensen PJ, Sun TT, Lavker RM. Involvement of follicular stem cells in forming not only the follicle but also the epidermis. Cell 2000;102:451–61.
12. Oshima H, Rochat A, Kedzia C, Kobayashi K, Barrandon Y. Morphogenesis and renewal of hair follicles from adult multipotent stem cells. Cell 2001; 104:233–45.
13. So PL, Epstein EH, Jr. Adult stem cells: capturing youth from a bulge? Trends Biotechnol 2004;22:493–6.
14. Ghazizadeh S, Taichman LB. Multiple classes of stem cells in cutaneous epithelium: a lineage analysis of adult mouse skin. EMBO J 2001;20:1215–22.
15. Morris RJ, Liu Y, Marles L, et al. Capturing and profiling adult hair follicle stem cells. Nat Biotechnol 2004;22:411–7.
16. Braun KM, Niemann C, Jensen UB, Sundberg JP, Silva-Vargas V, Watt FM. Manipulation of stem cell proliferation and lineage commitment: visualisation of label-retaining cells in wholemounts of mouse epidermis. Development 2003;130:5241–55.
17. Tani H, Morris RJ, Kaur P. Enrichment for murine keratinocyte stem cells based on cell surface phenotype. Proc Natl Acad Sci U S A 2000;97:10960–5.
18. Muller-Rover S, Handjiski B, van der Veen C, et al. A comprehensive guide for the accurate classification of murine hair follicles in distinct hair cycle stages. J Invest Dermatol 2001;117:3–15.
19. Morris RJ. Keratinocyte stem cells: target for cutaneous carcinogenesis. J Clin Invest 2000;106:3–8.
20. Stobbe CC, Park SJ, Chapman JD. The radiation hypersensitivity of cells at mitosis. Int J Radiat Biol 2002; 78:1149–57.
21. Bishop AJ, Kosaras B, Carls N, Sidman RL, Schiestl RH. Susceptibility of proliferating cells to benzo[*a*] pyrene-induced homologous recombination in mice. Carcinogenesis 2001;22:641–9.
22. Okamoto M, Yonekawa H. Intestinal tumorigenesis in Min mice is enhanced by X-irradiation in an age-dependent manner. J Radiat Res (Tokyo) 2005;46: 83–91.
23. Pazzaglia S, Mancuso M, Atkinson MJ, et al. High incidence of medulloblastoma following X-ray-irradiation of newborn Ptc1 heterozygous mice. Oncogene 2002;21:7580–4.
24. Calzada-Wack J, Kappler R, Schnitzbauer U, et al. Unbalanced overexpression of the mutant allele in murine Patched mutants. Carcinogenesis 2002;23: 727–33.
25. Suster S, Ramon y Cajal S. Myoepithelial differentiation in basal cell carcinoma. Am J Dermatopathol 1991; 13:350–7.
26. Mentzel T, Requena L, Kaddu S, Soares de Aleida LM, Sangueza OP, Kutzner H. Cutaneous myoepithelial neoplasms: clinicopathologic and immunohistochemical study of 20 cases suggesting a continuous spectrum ranging from benign mixed tumor of the skin to cutaneous myoepithelioma and myoepithelial carcinoma. J Cutan Pathol 2003;30:294–302.
27. Tsukamoto H, Hayashibe K, Mishima Y, Ichihashi M. The altered expression of α-smooth muscle actin in basal cell epithelioma and its surrounding stroma: with special reference to proliferating cell nuclear antigen expression and adenoid differentiation. Br J Dermatol 1994;130:189–94.
28. Karlsson L, Bondjers C, Betsholtz C. Roles for PDG-A and sonic hedgehog in development of mesenchymal components of the hair follicle. Development 1999;126: 2611–21.
29. Grachtchouk V, Grachtchouk M, Lowe L, et al. The magnitude of hedgehog signaling activity defines skin tumor phenotype. EMBO J 2003;22:2741–51.
30. International Agency for Research on Cancer: IARC Monograph on the Evaluation of Carcinogenic Risks to Humans. Vol. 55. Solar and Ultraviolet Radiation. IARC 1992.
31. United Nations Scientific Committee on the effects of atomic radiation, sources and effects of ionzing radiation. Vol. II: effects. Annex I. Epidemiological evaluation of radiation-induced cancer. New York: United Nations, 2000.
32. Wilson C, Cotsarelis G, Wei Z-G, et al. Cells within the bulge region of mouse hair follicle transiently proliferate during early anagen: heterogeneity and functional differences of various hair cycles. Differentiation 1994;55:127–36.
33. Miller SJ, Wei ZG, Wilson C, Dzubow L, Sun T-T, Lavker RM. Mouse skin is particularly susceptible to tumor initiation during early anagen of the hair cycle: possible involvement of hair follicle stem cells. J Invest Dermatol 1993;101:591–4.
34. Bickenbach JR. Isolation, characterization, and culture of epithelial stem cells. Methods Mol Biol 2005;289: 97–102.
35. Webb A, Li A, Kaur P. Location and phenotype of human adult keratinocyte stem cells of the skin. Differentiation 2004;72:387–95.
36. Li L, Mignone J, Yang M, et al. Nestin expression in hair follicle sheath progenitor cells. Proc Natl Acad Sci U S A 2003;100:9958–61.
37. Majka SM, Jackson KA, Kienstra KA, et al. Distinct progenitor populations in skeletal muscle are bone marrow derived and exhibit different cell fates during vascular regeneration. J Clin Invest 2003;111:71–9.
38. Amoh Y, Li L, Katsuoka K, Penman S, Hoffman RM. Multipotent nestin-positive, keratin-negative hair-follicle bulge stem cells can form neurons. Proc Natl Acad Sci U S A 2005;102:5530–4.
39. Pazzaglia S, Mancuso M, Tanori M, et al. Modulation of Patched-Associated susceptibility to radiation induced tumorigenesis by genetic background. Cancer Res 2004;64:3798–806.
40. Oro AE, Higgins KM, Hu Z, Bonifas JM, Epstein EH, Jr., Scott MP. Basal cell carcinomas in mice overexpressing sonic hedgehog. Science 1997;276: 817–21.
41. Sheng H, Goich S, Wang A, et al. Dissecting the oncogenic potential of Gli2: deletion of an NH(2)-terminal fragment alters skin tumor phenotype. Cancer Res 2002;62:5308–16.
42. Ikram MS, Neill GW, Regl G, et al. Gli2 is expressed in normal human epidermis and BCC and induces Gli1 expression by binding to its promoter. J Invest Dermatol 2004;122:1503–9.